Eurasia Journal of Science and Technology
Print ISSN: 2663-1024
Online ISSN: 2663-1016
DOI: https://doi.org/10.61784/ejst3148

RESEARCH PROGRESS ON CORROSION BEHAVIOR OF METALLIC URANIUM IN HUMID ATMOSPHERES

YiLi Sun*, Fei Wang
Rocket Force University of Engineering, Xi'an 710025, Shaanxi, China.
**Corresponding Author: YiLi Sun*

Abstract: The corrosion behavior of metallic uranium in humid environments is directly related to the safety and lifespan of nuclear facilities, but its microscopic mechanism has long been constrained by the spatiotemporal scale limitations of traditional density functional theory simulations. This paper systematically reviews the research progress of uranium corrosion in pure water, water-oxygen coexisting, and hydrogen environments. It points out that, limited by computational costs, traditional DFT struggles to reproduce the complex networks involving multi-molecule participation, multi-step reactions, and dynamic surface reconstruction during actual corrosion. This "common scale bottleneck" directly leads to controversies and blind spots regarding the core mechanisms in three key environments: the initial dissociation pathway of water molecules in pure water remains unclear; the "catalytic" acceleration effect of water in water-oxygen environments lacks support from microscopic kinetic landscapes; and the dynamic regulation mechanism of local strain on hydriding kinetics in hydrogen corrosion environments remains to be clarified. Combined with the latest theoretical simulation progress in the uranium-hydrogen system, this paper discusses how Machine Learning Interatomic Potentials, as a transformative tool, provides a new paradigm for bridging this scale gap by merging quantum mechanical accuracy with molecular dynamics efficiency. Finally, the paper looks to the future, pointing out that constructing high-fidelity MLIP for U-water and U-H systems to simulate the entire dynamic corrosion process under realistic surface morphologies and variable stress fields will be the key path to clarifying the controversial mechanisms and achieving a fundamental transition in uranium corrosion research from "static observation" to "dynamic prediction."
Keywords: Uranium; MLIP; Corrosion mechanism; Humid atmosphere

1 INTRODUCTION

The metal uranium (U), due to its extremely high density and unique nuclear properties, plays an irreplaceable role in the nuclear energy industry and national defense technology. Its performance stability is directly related to national strategic security and the long-term reliable operation of nuclear facilities [1-6]. However, uranium materials face a severe challenge in practical applications: their 5f electron configuration endows them with extremely high chemical activity, leading to very poor corrosion resistance in humid environments [7]. Even under trace water vapor conditions, the uranium surface corrodes rapidly [8], resulting not only in material loss but also in safety hazards due to hydrogen evolution from reactions [9-13]. Therefore, a deep understanding of the microscopic corrosion mechanism of uranium in humid atmospheres is the theoretical foundation for developing effective protection technologies and extending the service life of critical components.

Currently, atomic-scale theoretical simulation is a core means of revealing microscopic processes such as initial corrosion reactions and interface evolution. However, the depth of research in this field faces a fundamental bottleneck: traditional computational methods based on density functional theory (DFT), limited by their enormous computational cost, can only simulate system scales and time spans far smaller than those of actual corrosion processes. The corrosion behavior of uranium is a complex process driven by the synergy of material intrinsic factors and external environments, especially water vapor, hydrogen, and the synergistic effects of water and oxygen. It involves multi-physics coupling, including adsorption and dissociation of gas-phase molecules, ion migration through the oxide film, product nucleation and growth, and stress evolution. Traditional DFT simulations struggle to reproduce such complex dynamic reaction networks involving multiple molecules, multi-step reactions, and concomitant dynamic surface reconstruction. This "scale barrier" has directly led to long-standing controversies and difficulties in deepening the understanding of core mechanisms in three key environments: the exact dissociation pathway of water molecules on the uranium surface in pure water environments remains inconclusive; in water-oxygen coexisting environments, the "catalytic" acceleration effect exhibited by water molecules lacks support from a microscopic kinetic picture; in hydrogen corrosion environments, how local strain dynamically modulates hydrogenation kinetics remains a major blind spot.

To overcome the spatiotemporal scale constraints that limit the understanding of these mechanisms, machine learning interatomic potentials (MLIP) have recently emerged as a transformative tool. MLIP can learn and fit the potential energy surface of a system from high-precision DFT computational data using machine learning methods, thereby increasing computational efficiency by several orders of magnitude while maintaining near-DFT accuracy in atomic simulations. This makes it possible to simulate the entire dynamic corrosion process of uranium on near-realistic scales.

This article aims to systematically review the research progress on the corrosion behavior of metallic uranium in humid atmospheres. First, it analyzes the controversies over water dissociation mechanisms and catalytic effects in pure water

and water-oxygen coexisting environments, which arise from the insufficient scale of traditional DFT methods. Then, it extends the perspective to the "downstream effects" of water corrosion, exploring the mechanistic blind spots of stress-dynamics coupling in hydrogen corrosion. Finally, it looks forward to a future vision where constructing high-fidelity MLIP serves as the core strategy to achieve a fundamental transformation in uranium corrosion mechanism research from "static observation" to "dynamic prediction".

2 CORROSION OF METALLIC URANIUM IN PURE WATER ENVIRONMENT

2.1 Evolution of Kinetic Stages

The kinetic process of the uranium-water reaction exhibits distinct staged characteristics, and researchers have systematically characterized it using methods such as thermogravimetry, interferometry, and gas chromatography [14-17]. The current mainstream view holds that the kinetic process can be divided into two main stages:

Initial oxidation stage: In the early stage of the reaction, the fresh uranium surface rapidly adsorbs and dissociates water vapor, forming discrete island-like oxides, which then merge into a dense initial oxide layer (approximately 3 nm thick) [18]. The thickening of the oxide film in this stage is controlled by the diffusion rate of the oxidizing medium within the film, and the kinetics follow a parabolic law ($\Delta m^2 \propto t$). Kondo et al. [15], based on hydrogen evolution rate measurements, suggested that a logarithmic or exponential law may apply during a very short initial period.

Stable oxidation stage: This is the longest stage of the uranium-water reaction. Due to the significant density difference between metallic uranium and its oxide (UO_2), the growth of the oxide film generates enormous internal stress [19]. When the oxide film thickness reaches a critical value (70-600 nm) [20, 21], the internal stress reaches a critical value (approximately 1.93 GPa) [22], leading to cracking and spalling of the film, which becomes loose and flaky. At this point, the growth and rupture/spalling of the oxide film reach a dynamic equilibrium, maintaining a protective film of constant thickness at the interface. The corrosion weight gain or hydrogen evolution rate shows a linear relationship with time ($\Delta m \propto t$) [17]. Due to the limitations of early measurement techniques, a large amount of data in the existing literature focuses on this linear stage.

During the stable linear stage, the corrosion rate (k) of metallic uranium is primarily controlled by the ambient temperature (T) and water vapor pressure (P). Experimental data confirm that over a wide pressure range (0.01-101.325 kPa) [23], the corrosion rate in the linear stage is proportional to the square root of the water vapor pressure, i.e., $k \propto P^{0.5}$. This characteristic is typically attributed to the Langmuir chemisorption mechanism of water vapor on the uranium/uranium oxide surface [24]. Meanwhile, the temperature dependence of the corrosion rate follows the Arrhenius equation [25].

The reaction mechanism of the U-H_2O system is similar to that of the U-O_2 system, both producing slightly hyperstoichiometric UO_{2+x}. Moreover, the corrosion rate of the U-H_2O system is much higher than that of the U-O_2 system, potentially by several orders of magnitude [26]. In the early stage of oxidation, the corrosion rate of uranium follows a parabolic law; after the surface oxide layer forms and grows, the corrosion behavior transitions to linear or quasi-linear kinetics (as shown in Fig. 1) [27]. As with any other metal, the oxidation of uranium is expected to continue until the entire metal is consumed, provided the supply of oxidizing species is sufficient. When the metal is completely consumed, the oxidation rate is expected to level off, reaching zero-order kinetics. The chemical reaction equation is as follows: $U + (2+x)H_2O \rightarrow UO_{2+x} + (2+x)H_2$. Due to the fast reaction rate and complex nature of the system, researchers have not yet reached a unified conclusion on whether water completely dissociates into $2H^+$ and O^{2-} on the uranium surface or partially dissociates into H^+ and OH^- (as shown in Fig. 2).

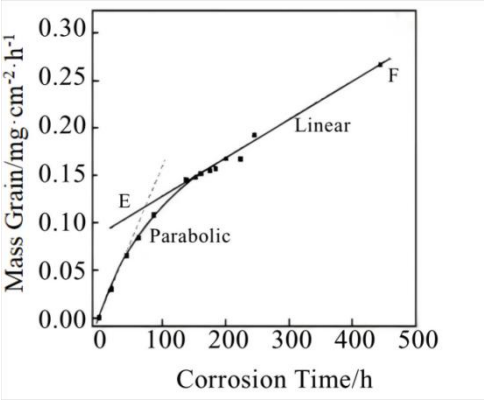

Figure 1 Corrosion Rate of Metallic Uranium in Water [27]

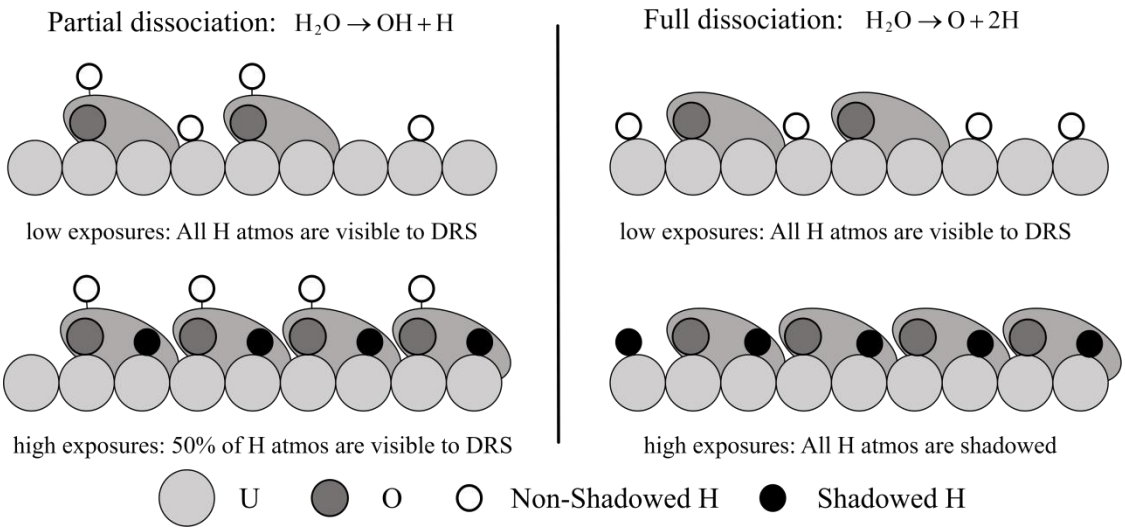

Figure 2 Two Pathways of Adsorption on the Uranium Surface at Room Temperature [28]

2.2 Complete Dissociation

Experimental studies: Shamir et al. used a shadowing model established by Direct Recoil Spectroscopy (DRS) to point out that on the U surface [28], H_2O molecules tend to follow the Langmuir mechanism and undergo complete dissociation ($H_2O \rightarrow O^{2-} + 2H^+$) [24]. Manner et al. suggested that at very low coverages (below 0.5 L) [29], water undergoes complete dissociation, leaving surface-bound oxygen atoms, which then react with chemisorbed water to form hydroxyl groups. Winer et al. using X-ray Photoelectron Spectroscopy (XPS) [8], also found a shift in the O 1s peak, indicating that adsorbed H_2O completely dissociates, and the generated O^{2-} rapidly reacts with U to form island-like UO_2. Santon et al. proposed that the reaction of uranium with water vapor below 230 °C is a diffusion-controlled system [20]. After the oxide layer partially cracks at 70 nm, it becomes an oxide layer of constant thickness. Based on the diffusion coefficient, they assumed that O^{2-} is the only diffusing species. After the initial parabolic stage, the reaction becomes linear, with the following assumptions: at the metal-oxide interface: $U \rightarrow U^{4+} + 4e^-$, and at the gas-oxide interface: $2H_2O + 4e^- \rightarrow 2O^{2-} + 2H_2$. Moreover, Santon considered that the behavior of hydrogen may be more complex [20]. Through the above process, negative charge accumulates at the oxide-metal interface, which inhibits further diffusion of O^{2-} through the metal. Therefore, the dissociation mode of water at the gas-oxide interface is as follows: $H_2O \rightarrow O^{2-} + 2H^+$. The protons in the equation are likely to partially diffuse through the voids of the cationic surfactant to the oxide-metal interface to neutralize the negative charge, thereby allowing oxygen ions to diffuse. The role of hydrogen in the reaction may increase due to the mechanical failure of the oxide layer.

Theoretical calculations: Liu investigated the adsorption behavior of H_2O molecules on the α-U (001) surface based on first-principles calculations [30]. The study shows that configurations with H-terminated ends are difficult to stabilize. The most stable molecular adsorption configuration is H_2O adsorbed in a parallel top site on the surface. H_2O can spontaneously dissociate on the U surface into $H^+ + OH^-$ or $O^{2-} + 2H^+$. Moreover, the adsorption energies of both complete and partial dissociation configurations are significantly higher than those of molecular adsorption, indicating that complete dissociation is thermodynamically most stable. Electronic structure analysis further confirms that the bonding strength between the dissociation products and uranium is stronger than that of the intact H_2O molecule. Zhu et al. reached similar conclusions on the γ-U (001) and (100) surfaces [31, 32]. On the γ-U (001) surface, H_2O also prefers parallel top-site adsorption. The dissociation barrier of H_2O is much lower than the adsorption energy, and the entire process is highly exothermic, indicating that dissociation occurs very readily [31]. On the γ-U (100) surface [32], the adsorption energies for molecular adsorption, partial dissociation, and complete dissociation are 2.28 eV, 3.23 eV, and 4.32 eV, respectively, with complete dissociation being the most favorable. Stepwise dissociation path analysis (as shown in Fig. 3) reveals that both the initial and complete dissociation steps are exothermic reactions with very low energy barriers (0.52 eV and 0.22 eV, respectively). Furthermore, in a multi-molecule environment, the dissociation barrier decreases further: when two water molecules coexist, the dissociation barrier is only 0.07 eV, releasing 1.89 eV of heat; with four water molecules, the dissociation barrier disappears completely [32], indicating that intermolecular synergistic effects are crucial.

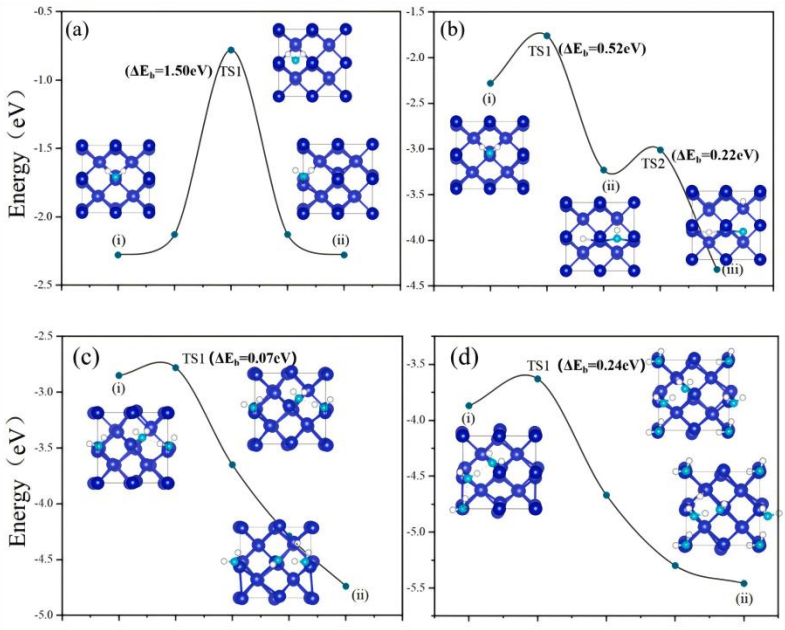

Figure 3 Water Dissociation Energy Barrier [32]

2.3 Partial Dissociation

Experimental studies: Shamir et al. found that when the oxide film coverage on the U surface exceeds 60% [28], the adsorbed H_2O molecules are more likely to undergo only partial dissociation, generating OH^- and H^+. Balooch using Temperature Programmed Desorption (TPD) [33], further confirmed that OH^- from partial dissociation can be detected on both U and uranium oxide surfaces. In addition, Danon et al. also used TPD to study mildly and heavily oxidized U samples [34], suggesting that water molecules may undergo reversible chemisorption and partial dissociation at weak binding sites on the U surface. Baker et al. proposed that OH^- is the diffusing species [26]. This view is supported by the identification of hydrides in the reaction products and by the higher reaction rate compared to dry oxygen under the same conditions. Baker's mechanism indicates that water undergoes partial dissociation on the oxide surface [26]: $H_2O \rightarrow OH^- + H^+$, while at the metal-oxide interface: $H^+ + e^- \rightarrow H\cdot$. Subsequently, H has two reaction paths: reacting with U at the metal-oxide interface: $3H\cdot + U \rightarrow UH_3$ or diffusing to the gas-oxide interface to form molecular hydrogen: $2H\cdot \rightarrow H_{2(g)}$.

Theoretical calculations: Li studied the adsorption, diffusion, and dissociation of H_2O on the α-U (001) surface using generalized gradient density functional theory [35]. The most stable configuration remains top-site adsorption parallel to the surface, with an adsorption energy of 0.58 eV. The main mechanism originates from the spatial overlap of the H_2O 1b1 orbital with the uranium 6d orbital, accompanied by weak overlap of the 3a1 orbital (a π orbital formed by O 2py and H 1s) with the U 6d orbital. The diffusion barrier of H_2O between adjacent top sites is 0.20-0.23 eV, indicating that surface migration is facile. The dissociative adsorption of OH+H is 1.24-1.39 eV higher in energy than molecular adsorption, and the dissociation barrier is 0.56-0.62 eV, suggesting that under appropriate thermal activation, adsorbed water molecules tend to dissociate into OH^- and H atoms.

3 CORROSION OF METALLIC URANIUM IN A WATER-OXYGEN MIXED GAS

In actual storage environments, metallic uranium rarely encounters absolutely dry oxygen or pure water vapor; instead, it is more often exposed to a water-oxygen mixed atmosphere. The corrosion kinetics of metallic uranium in a H_2O-O_2 mixture are similar to those in pure oxygen or pure water vapor systems, macroscopically characterized mainly by a brief initial parabolic stage followed by a long-term linear stage [36]. In the parabolic stage, the corrosion rate decreases with time; after entering the linear stage, the weight gain becomes linear with time. During the corrosion process of metallic uranium in H_2O-O_2, water molecules act as a "catalyst". Specifically, in the early stage when O_2 and H_2O coexist, metallic uranium preferentially reacts with O_2, and water molecules only participate in regulating the reaction process without being consumed themselves (as shown in Fig. 4); only when oxygen is nearly completely consumed (the critical value is approximately $P_{O_2} = 2Pa$, which depends on conditions such as temperature), no hydrogen is produced during this process. When the oxygen partial pressure falls below this critical value, water molecules then react as a reactant with metallic uranium, and the reaction rate of U begins to increase. At this point, the reaction rate becomes entirely dependent on the water vapor pressure, and H_2 begins to be generated [37]. The discovery of this "catalytic" mechanism provides important clues for understanding the phenomenon of accelerated corrosion of metallic uranium by H_2O-O_2, but a clear theoretical explanation of how water molecules influence the corrosion reaction pathway and rate through microscopic interactions is still lacking.

3.1 Experimental Studies

The corrosion of uranium in H_2O-O_2 is a complex process influenced by multiple environmental factors [38-41]. Studies have shown that water significantly accelerates the corrosion rate of uranium (as shown in Fig. 5) [41]. Experimental data indicate that under the same temperature and pressure conditions, the corrosion rate of uranium in H_2O-O_2 can be 2-5 times higher than that in a pure oxygen environment [41]. Humidity and temperature are important factors affecting the corrosion kinetics. Furthermore, the composition of corrosion products of U in H_2O-O_2 is also more complex. In addition to typical uranium oxides (e.g., UO_2 and UO_3), it is often accompanied by the formation of uranium hydroxides (e.g., $U(OH)_4$) or hydrated uranium oxides (e.g., $U_3O_8 \cdot nH_2O$). Existing experimental observations show that at low temperatures (e.g., 0–75 °C) [42], humidity can significantly accelerate corrosion, and both temperature and humidity also affect the ductility of uranium, with the degree of influence related to factors such as surface oxidation, heat treatment, and specimen shape. Recent research has utilized X-ray Diffraction (XRD) to study the surface oxidation of uranium metal in air at 50–300 °C, establishing the kinetic expression for the formation of UO_2.

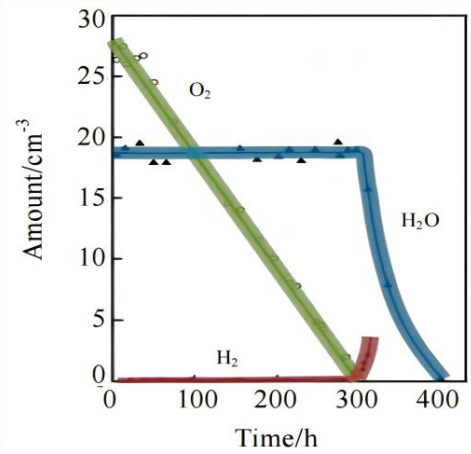

Figure 4 Relationship Between Corrosion Products and Time [37]

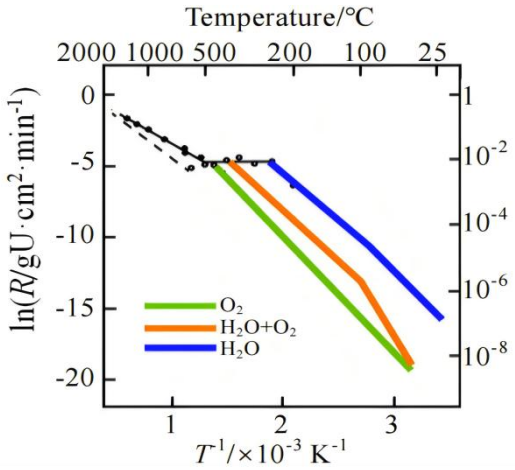

Figure 5 Corrosion Rate of Uranium Metal [41]

Early research on the corrosion mechanism of uranium in H_2O-O_2 was not in-depth, and it was once believed that the corrosive medium was single. For example, Haschke compared the corrosion kinetics data and corrosion product characteristics of uranium in dry air [43], water vapor, and humid air, and proposed that O^{2-} is the only diffusing medium. He suggested that H from H_2O does not enter the oxide lattice but adsorbs on the oxide surface and recombines with O_2 to form H_2O, i.e., water-catalyzed oxidation. Colmenares and Weirick et al. proposed that corrosion primarily originates from O^{2-} generated by O_2 dissociation [44,45], and that water vapor only increases microdefects in the corrosion product. O_2 enters the oxide lattice as O^{2-} and diffuses via an interstitial mechanism. Kondo et al. argued that the introduction of water vapor generates H atoms or H_2 [15], which then form hydrides; hydrides act as intermediates to increase the reaction rate, so the presence of water promotes the corrosion process to a certain extent. However, these views were later overturned by the isotopic tracer experimental results of Baker et al. [46]. That experiment showed that OH^- is the main medium in the diffusion process, and O_2 does not directly participate in the reaction but combines with hydrogen in the corrosion product to form water. Colmenares et al. further pointed out that water vapor synergizes with oxygen to form OH^- in the oxide lattice [47], thereby accelerating corrosion. McGillivray et al. used secondary ion mass spectrometry with isotopic labeling of ^{18}O to analyze the isotopic composition of the oxide in depth. When $H_2{}^{18}O$ was labeled [48], the proportion of ^{18}O in the oxide layer was 70–75%, proving that water

molecules participate in the reaction and contribute the main oxygen source. When $^{18}O_2$ was labeled, ^{18}O was still detected, indicating that oxygen also directly participates in the oxidation process. Based on this, McGillivray pointed out that oxidation is driven by the co-diffusion of O^{2-} from O_2 and OH^- from H_2O, rather than a single pathway. The adsorption of H_2O occurs on top of the pre-adsorbed oxygen layer, suppressing hydrogen generation. This view is now widely accepted in the scientific community. Based on this co-medium mechanism, Allen et al. further proposed a microchannel transport model for the corrosive medium [18]: when the thickness of the oxide film on the uranium surface exceeds 3 nm, the diffusion of corrosive media (OH^-, O^{2-}, O, etc.) is mainly controlled by microchannels in the oxide film. Among these, the transport rate of OH^- is higher than that of O^{2-} and does not significantly affect the transport efficiency of O^{2-} . When the oxygen content is high, oxygen transport dominates in the microchannels, and the promoting effect of water is not obvious; under low-oxygen conditions, OH^- transport can still proceed effectively.

3.2 Theoretical Calculations

Theoretical calculations: Existing theoretical studies have mostly focused on the initial reaction step of co-adsorption of water and oxygen. Skomurski et al. investigated the co-adsorption behavior of H_2O and O_2 on the stable $UO_2(111)$ surface [49]. They found that when water molecules and oxygen atoms are co-adsorbed on the UO_2 surface, the presence of water significantly lowers the energy barrier for uranium oxidation compared to simple oxygen adsorption under dry conditions. The key mechanism is that adsorption of polar water molecules induces changes in the electronic structure in the near-surface region of UO_2; this subtle adjustment makes it easier for the adsorbed oxygen atoms to transition from a high-spin state to a low-spin state, thereby greatly promoting charge transfer between the oxygen atoms and surface uranium atoms and triggering uranium oxidation. By calculating the adsorption energies for different spin configurations, Skomurski quantitatively compared the oxidation pathways under dry and wet conditions [49]. The results show that, in the presence of water, the activation energy for the oxidation process decreases from 1.66 eV under dry conditions to 0.50 eV. According to the Boltzmann equation, this reduction in energy barrier makes the oxidation rate on the $UO_2(111)$ surface change from negligible to almost instantaneous. Qu Xin et al. systematically studied two co-adsorption mechanisms of O_2 and H_2O on the UO_2 surface [50, 51]. The first mechanism involves the co-adsorption of O_2 and H_2O molecules on the surface, as shown in Fig.6. Calculations show that O_2 significantly promotes the dissociation of H_2O, and the smaller the distance between them, the stronger the promoting effect. The dissociation process consists of two steps.

First, the co-adsorbed O_2 molecule strongly attracts a hydrogen atom in the nearby H_2O, causing the hydrogen to move toward O_2 and leading to breakage of the H-O bond; then, the hydrogen atom generated by dissociation interacts with the UO_2 surface, causing O_2 to decompose into two oxygen atoms, one of which combines with hydrogen to form an OH group. Subsequently, the dissociated O atom and the OH group diffuse to stable adsorption sites on the surface, completing the dissociation process.

The second mechanism is that O_2 preferentially adsorbs on the surface (as shown in Fig.7), which also greatly enhances the dissociation tendency of H_2O. The subsequently adsorbed H_2O molecule first reorients from vertical to horizontal. Under the joint attraction of the pre-adsorbed oxygen atom and surface atoms, one of its H-O bonds breaks, generating a hydrogen atom and an OH group; this hydrogen atom then combines with a pre-adsorbed oxygen atom to form a new OH group, while the original OH group diffuses toward a bridge site.

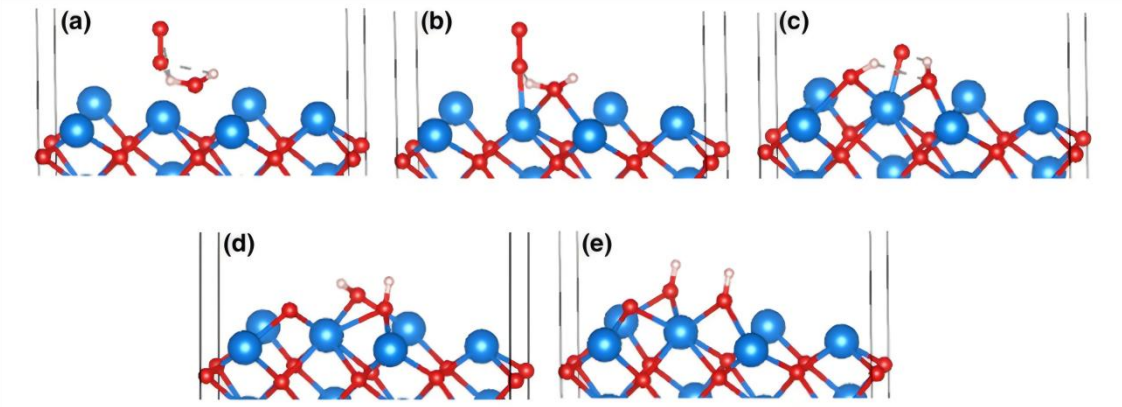

Figure 6 Dissociation Pathway of H_2O and O_2 Co-adsorption [50]

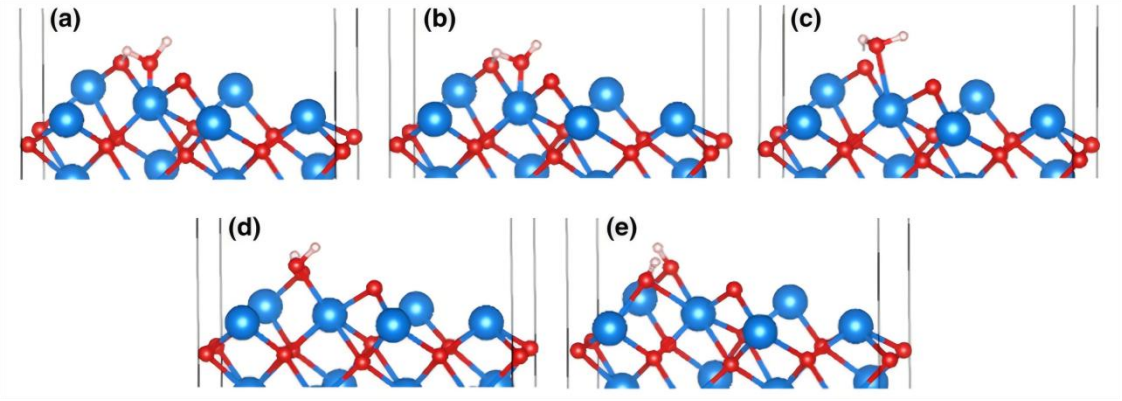

Figure 7 Dissociation Pathway of O_2 Pre-adsorption [50]

The above analysis indicates that the promoting mechanism in the early stage of the reaction mainly originates from the strong attraction of oxygen atoms to the hydrogen in H_2O, thereby pulling the hydrogen atom out of the H_2O molecule. However, how H_2O affects the pathway and rate of the corrosion reaction through microscopic interactions i.e., the specific details of its "catalytic mechanism" has not yet been fully elucidated.

The root of the above research bottleneck can be largely attributed to the scale limitations faced by current theoretical calculations. Limited by the inadequacies of simulation systems in both spatial and temporal dimensions, existing models struggle to fully reproduce the complex reaction networks involving multiple molecules, multiple steps, and long-range cooperation that occur in actual corrosion processes. The lack of computational scale often leads to the simplification or neglect of key intermediate states, structural reconstructions, and dynamic evolution pathways, thereby undermining the authenticity and predictive power of computational results.

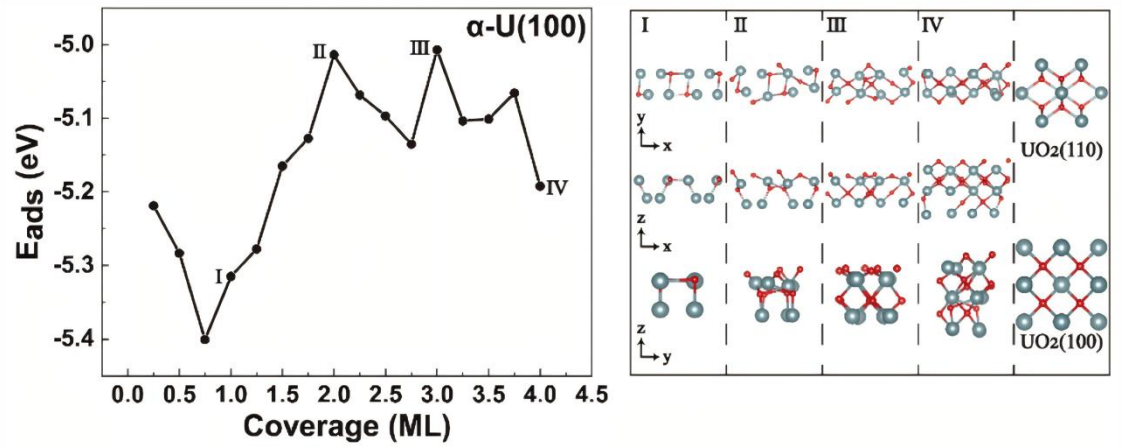

Figure 8 Adsorption Energy and Adsorption Configuration of O Atoms on α-U(100) at Different Coverages [52]

Taking the oxidation process of α-U as an example [52]: As shown in Fig. 8, the initial oxidation behavior of its (100) surface is significantly influenced by oxygen atom coverage. At low coverage (<0.75 ML), O atoms mainly occupy surface hollow sites, and the relaxation of surface uranium atoms is not obvious. As the coverage increases (0.75-2 ML), the adsorption energy decreases nearly linearly. At 1 ML, O atoms and surface U atoms arrange to form a surface structure with a U:O ratio of 1:1 (as shown in Fig. 8 I). When the coverage exceeds 2 ML, the original highly symmetric structure (e.g., at 1 ML) disappears. The surface undergoes undulating reconstruction, with some O atoms diffusing into the subsurface, gradually forming structurally complex intermediate phases of uranium oxide (II, III, IV). Especially under full coverage (e.g., 3 ML), the surface structure approaches that of the UO_2(100) surface, indicating that the initial oxidation of the α-U(100) surface tends to ultimately form the UO_2(100) surface. Thus, studying only the adsorption of a single oxygen atom cannot fully reveal the structural evolution during the oxidation process.

A similar phenomenon also occurs on the γ-U(100) surface [52]. As the oxygen coverage increases from 1 ML to 3 ML, this surface successively undergoes the formation of an ordered UO layer, the construction of an O-U-O three-dimensional framework, significant surface relaxation, and energy fluctuations of about 0.37 eV, ultimately leading to spallation of the oxide layer due to a lattice mismatch of up to 57.9% between the oxide layer and the substrate. This series of changes encompasses various complex mechanisms including surface reconstruction, atomic embedding, and interlayer expansion.

If the computational scale is limited, it is difficult to fully simulate such dynamic oxidation pathways accompanied by significant structural relaxation, let alone effectively bridge the cross-scale mechanisms from initial adsorption to bulk corrosion. Therefore, insufficient computational scale has become a key obstacle restricting in-depth research on the corrosion behavior of uranium in H_2O-O_2.

4 CORROSION OF METALLIC URANIUM IN H_2

Hydrogen generated by the uranium-water reaction is one of the important sources of external hydrogen in uranium materials. The reaction process is:

$$U + (2 + x)H_2O \rightarrow UO_{2+x} + (2 + x)H_2$$

In a pure water vapor environment, the corrosion process of metallic uranium is accompanied by the release of hydrogen gas and the formation of surface oxides. At the same time, the hydrides formed by corrosion can further react with water vapor to generate oxides and release hydrogen gas. The generated hydrogen gas partially dissociates into active hydrogen atoms on the uranium surface and is adsorbed; these atoms subsequently penetrate into the uranium metal lattice, leading to the formation of hydrides such as uranium hydride (UH_3). Since the density of the hydride is much lower than that of the metal matrix, its formation is accompanied by significant volume expansion, inducing stress within the material, which in turn leads to microcracks, pulverization, and even structural collapse. Therefore, the study of uranium-water corrosion naturally leads to an in-depth investigation of its “downstream effects”, which are directly related to the long-term structural integrity and safe service performance of uranium materials in hydrogen-containing environments.

4.1 Evolution of Kinetic Stages

For metallic uranium with a pre-oxidized surface, the hydriding reaction process typically exhibits characteristic stages, generally divided into three consecutive stages: the induction period, the nucleation and growth of UH_3 sites, and the bulk reaction stage [53, 54]. On a mildly oxidized metal surface, the initial development of hydrides usually appears as discrete, growing “spots” [55-60]. For a hydride spot to nucleate, the hydrogen flux at the metal surface must exceed the hydrogen flux diffusing into the bulk metal, thereby achieving local saturation [61, 62]. Since both fluxes vary exponentially with temperature, if the gas pressure is insufficient, the nucleation rate may be limited [62]. The number density of hydride spots is finite, depending primarily on the solubility of H_2 in the metal and the metal's microstructure [57]. If a sufficient hydrogen source is available, the nucleation centers tend to grow radially and eventually form a continuous hydride layer on the metal surface. This layer then thickens via a "shrinking core" morphology, ultimately consuming the entire metal [63, 64].

It is now generally accepted that before hydride nucleation, hydrogen must penetrate the passive oxide layer on the metal surface; this process is termed the induction period [53, 57, 65]. When hydrogen permeates through the oxide layer, it tends to accumulate at the oxide-metal interface. When the hydrogen concentration in the metal at this interface exceeds the solubility limit of the hydride, the gas-solid hydriding reaction occurs. The hydrogen concentration at the interface depends on the net balance between the input flux of hydrogen atoms crossing the oxide-metal boundary and the output flux diffusing into the metal substrate. For surface-oxidized uranium, the hydrogen accumulation process prior to hydride formation can be summarized by the following basic steps [66]:

Surface adsorption: Physical adsorption of H_2 on the oxide surface, followed by dissociation into two H atoms or ions for diffusion or chemisorption.

Permeation diffusion: Hydrogen, either as molecules or, after dissociation, as atoms/ions, penetrates and diffuses through the oxide layer covering the metal surface toward the interior.

Concentration buildup: Hydrogen atoms accumulate at the oxide-metal interface until the concentration reaches the hydride solubility limit, triggering the reaction.

Cohen et al. developed a model that combines diffusion characteristics and surface properties to quantitatively describe the first two steps [67]: the adsorption step is described as a function of the sticking probability on the oxide film surface and the desorption rate constant; the permeation step is controlled by the oxide film thickness and the diffusion rate constant. If uranium is exposed to an atmosphere containing hydrogen, oxygen, and water vapor simultaneously, the reaction induction period is significantly prolonged and the reaction rate is suppressed [58, 68]. This is because oxidation enhances the surface passive layer, or because oxygen and water vapor compete with hydrogen for surface adsorption sites [62, 69]; at the same time, they may saturate the oxide layer, block diffusion channels [70], or generate competing anions [71], thereby hindering the hydriding reaction. First-principles calculations provide atomic-scale insight into this complex process from induction to phase transformation. Taylor et al.[72, 73], based on DFT calculations, revealed the microscopic mechanism of the α-U to UH_3 phase transformation. They found that the formation of a hydrogen-saturated α-U phase is the rate-limiting step for hydride nucleation, and the accompanying volume expansion constitutes the main energy barrier. Once saturation is reached, the subsequent transformation to α-UH_3 has no significant kinetic barrier. This theoretical finding perfectly explains the induction period behavior observed in experiments and the key role of hydrogen concentration buildup in triggering the phase transformation.

4.2 Nucleation Sites and Grain Boundary Hydrogen Behavior

The initial growth of hydrides on the uranium surface typically begins at discrete, isolated points or regions [56], indicating that specific surface sites have higher reactivity toward the hydriding reaction [74], and these nucleation sites are mainly located at the metal-oxide interface [75]. The prerequisite for hydride phase precipitation is that the local hydrogen concentration in the metal exceeds its solubility limit. Taking the natural uranium-hydrogen system as an example, the surface oxide layer exhibits spatial inhomogeneity in composition and thickness, and is often accompanied

by defects, microcracks, and topographical undulations. This microstructural heterogeneity leads to differences in the physical adsorption of hydrogen on the surface and in its permeation through the oxide layer, thereby forming local "active" regions. In these regions, hydrogen can accumulate more rapidly and reach a critical concentration, inducing preferential nucleation [76]. Based on growth rates and specific nucleation sites [56], four typical nucleation types have been identified, which are closely related to surface damage, point defects, inclusions, and crystal defects [56, 62]. Notably, the metallic lattice defects that provide nucleation sites (such as grain boundaries and inclusions) are strongly linked to the structural integrity of the overlying oxide layer [77, 78].

Among the numerous defect sites, grain boundaries are preferential locations for hydride nucleation, particularly in high-purity metals with a low density of inclusions. Studies have shown that grain boundaries generally exhibit higher hydrogen diffusion coefficients than the grain interior, providing diffusion channels for hydrogen to enter the subsurface of the metal [79]. Meanwhile, grain boundaries that intersect the surface at an acute angle exhibit higher activity due to their large exposed area and geometric favorability for rapid accumulation of hydrogen at the wedge tip [80]. Furthermore, the oxidation rate in the early stage of metal oxidation is orientation-dependent [78]. Differences in oxidation rates among grains of different orientations induce stress at oxide-oxide interfaces, causing structural discontinuity of the oxide layer at grain boundaries, which further enhances hydrogen permeation capability [81].

In response to the above experimental observations, Li et al. used first-principles calculations to elucidate at the atomic scale the mechanisms of preferential hydrogen segregation at grain boundaries and the initiation of hydrogen embrittlement [82]. Their study of three typical symmetric tilt grain boundaries in uranium showed that the grain boundary structure significantly affects hydrogen behavior: the higher the grain boundary energy, the stronger the trapping capability for hydrogen atoms. Hydrogen atoms tend to diffuse horizontally within the grain boundary region and have difficulty penetrating into the grain interior. Electronic structure analysis reveals that the uranium 6d orbitals and hydrogen 1s orbitals hybridize to form bonds at the grain boundary. Furthermore, first-principles tensile tests confirm that the U-H bonds formed by hydrogen dissolution lead to a significant decrease in electron density and bonding strength of adjacent critical intergranular U-U bonds across the grain boundary. This is the fundamental cause of hydrogen embrittlement at uranium grain boundaries and also theoretically explains why hydrides tend to nucleate at defects such as grain boundaries.

After initial nucleation at active sites, the subsequent growth dynamics of hydrides are strongly regulated by stress and the integrity of the oxide layer. Experimental observations have revealed that before the formation of macroscopically visible hydride spots, submicron-scale hydride nuclei often form and grow. If the volume expansion of a nucleus is insufficient to rupture the overlying oxide layer, a compressive stress field develops that intensifies as the nucleus grows, leading to growth retardation or even deceleration. If the oxide layer remains intact, nucleus growth stalls at a certain critical size (typically less than 3-4 μm), forming so-called "small-size" precipitate colonies [83]. Conversely, if a growing hydride nucleus ruptures the oxide layer, the compressive stress is relieved, and growth is no longer mechanically constrained by the oxide layer, thereby entering a rapid growth stage and forming typical "large-size" precipitate colonies. This indicates that the final morphology and growth rate of hydrides are essentially the result of a dynamic interplay between local hydrogen concentration buildup and the stress field.

4.3 Bulk Reaction and Stress Effects

As individual hydride sites undergo linear lateral growth and eventually coalesce [57], the metal surface gradually becomes completely covered by hydride. Once the surface sites merge into a continuous layer, the bulk reaction begins, and the kinetic mode transitions to a decelerating linear relationship [84], with the reaction front advancing into the metal interior. Under steady-state conditions, the UH_3 layer propagates into the bulk metal at a constant velocity, maintaining a fixed adherent thickness. Due to the significant volume expansion and lack of coherency between the hydride product and the metal matrix, the reaction induces stress cracking, leading to spallation of the hydride along planes parallel to the metal surface. At the nanoscale, this volume-expansion-induced cracking of the parent metal, in turn, provides pathways for hydrogen ingress, thereby accelerating local reactions [85].

Uranium materials may be subjected to internal, external, surface, and interfacial stresses during manufacturing [86, 87], machining [88], and even corrosion processes [89]. Depending on the source and stage, these stress-induced strains can be mainly summarized as: internal strains introduced by thermal processing during fabrication, external strains remaining after mechanical working, and corrosion-induced strains generated during oxidation and hydriding. Some DFT studies suggest that internal tensile or expansive strains may promote UH_3 formation, whereas compressive strains may inhibit the reaction [72, 73]. Experiments by Stitt et al. have also observed that UH_3 preferentially forms at geometric tips with high tensile stress [90]. However, how strain specifically regulates hydriding kinetics, particularly its influence in practical engineering applications, remains unclear. This is because traditional DFT calculations are limited by system size and cannot simulate the dynamic coupling of stress with multiple processes such as hydrogen diffusion and hydride nucleation and growth, while experiments struggle to isolate strain effects at the atomic scale.

4.4 Advances in Theoretical Simulation and Future Challenges

To explore the microscopic mechanism of the uranium hydriding reaction, significant progress has been made in theoretical simulation studies in recent years. In addition to the aforementioned research on phase transformation mechanisms and grain boundary behavior, Liu Min systematically investigated the structural evolution of

uranium-hydrogen compounds under pressures ranging from 0 to 300 GPa using crystal structure prediction algorithms combined with first-principles calculations [91]. They predicted 20 uranium hydrides (including seven new structures) and found that hydrogen-rich phases exhibit potential superhard characteristics due to enhanced covalent bonding under high pressure, providing a basis for understanding uranium-hydrogen behavior under extreme conditions. Chen et al. [92] combined computational and experimental approaches to systematically study the mechanism by which niobium improves the hydrogen corrosion resistance of uranium-niobium alloys. They found that niobium influences hydrogen behavior in distinctly different ways in dilute and concentrated alloys by forming hydrogen traps or "Nb-influenced channels," and that the growth of the resulting hydride (β-UH_3) expels niobium atoms to form a Nb-rich layer, producing a self-limiting effect. In terms of potential development, the ChIMES reactive force field model developed by Soshnikov et al. [93], parameterized by fitting DFT data, can accurately reproduce the basic physical properties of α-U, α-UH_3, and β-UH_3, and precisely predict defect formation energies and hydrogen diffusion barriers. The computational efficiency of this model is much higher than that of DFT, providing a highly efficient and accurate preliminary tool for studying the uranium hydriding mechanism on larger spatiotemporal scales.

However, in addressing the key scientific question of how strain dynamically and coupledly regulates hydriding kinetics, existing first-principles calculations are limited by scale, while empirical potentials may lack the accuracy to describe the complex coupled process of stress-diffusion-chemical reaction. Developing a high-fidelity MLIP for the U-H system is a critical pathway to overcome this bottleneck. MLIP can achieve large-scale, long-time molecular dynamics simulations containing realistic surface morphologies, grain boundary structures, and variable stress fields with near-DFT accuracy. Using MLIP, one can simulate the diffusion pathways of hydrogen atoms under stress fields, the nucleation and growth of hydrides at stress concentrations, and the dynamic feedback mechanism between stress and the corrosion reaction. This will allow direct resolution of the microscopic picture of strain-regulated hydriding kinetics from atomic trajectories, providing a revolutionary theoretical tool for understanding the hydrogen corrosion behavior of uranium under complex engineering environments and predicting its long-term safety.

5 CONCLUSION

The study of the corrosion mechanism of metallic uranium in humid environments is undergoing a profound transformation from macroscopic phenomenon observation to microscopic mechanism analysis. This article systematically reviews the progress in computational simulation studies of uranium corrosion in pure water, water-oxygen coexisting environments, and hydrogen atmospheres, and points out that the fundamental challenge currently facing this field stems from the severe spatiotemporal scale limitations of traditional theoretical simulation methods. Constrained by enormous computational costs, conventional DFT calculations struggle to reproduce the complex networks involving multiple molecules, multi-step reactions, and concomitant dynamic surface reconstruction that occur in actual corrosion processes. This "common scale bottleneck" has directly led to controversies and blind spots regarding the core mechanisms in three key environments: in pure water, the initial dissociation pathway of water molecules on the uranium surface remains unclear; in water-oxygen coexisting environments, the "catalytic" effect of water molecules lacks atomic-scale microscopic picture support; in hydrogen corrosion environments, the dynamic regulation mechanism of local strain on hydriding kinetics has yet to be clarified.

To completely move beyond the stage of simplified static models in understanding key mechanisms, the research frontier must shift toward seeking a new paradigm that balances quantum mechanical accuracy and molecular dynamics efficiency. Future research on the corrosion behavior of uranium in humid atmospheres is recommended to focus on the following three dimensions:

(1) Construct a high-fidelity MLIP for the U-H_2O system to resolve fundamental controversies. In response to the fundamental controversy over the water dissociation mechanism in pure water, there is an urgent need to develop a dedicated MLIP for the U-H_2O system. By simulating the interaction of water molecules with large systems possessing realistic surface morphologies on the nanosecond timescale, the dissociation pathways and probabilities can be statistically analyzed, providing direct atomic-scale evidence for the controversy.

(2) Use MLIP to dynamically resolve the microscopic picture of water "catalysis". To address the lack of detail on the catalytic mechanism in the H_2O-O_2 environment, MLIP can be used to simulate the entire process of co-adsorption, reaction, and ion transmembrane diffusion of water and oxygen molecules on dynamically evolving surfaces. MLIP has already demonstrated excellent capability in handling multi-molecule environments in studies of oxide-water interfaces such as hematite [94], rutile TiO_2 [95], and MgO [96], achieving dynamic process simulations with computational efficiency thousands of times higher than conventional DFT. Drawing on these achievements, the catalytic role of water molecules in uranium corrosion can be directly interpreted from atomic trajectories.

(3) Extend the MLIP for the U-H system to reveal the coupling mechanism between stress and hydriding kinetics, as well as data gaps. Regarding the influence of local strains induced by manufacturing, processing, and irradiation on hydrogen corrosion, existing DFT and empirical potentials cannot describe the complex "stress-diffusion-phase transformation" coupling process. Constructing an MLIP for the U-H system is a key pathway to simulate hydrogen atom diffusion under stress fields, hydride nucleation in stress-concentrated regions, and dynamic feedback mechanisms, thereby providing a revolutionary theoretical tool for understanding the hydrogen corrosion behavior of uranium under complex engineering environments.

COMPETING INTERESTS

The authors have no relevant financial or non-financial interests to disclose.

REFERENCES

[1] Aristova NM, Belov GV, Morozov IV, et al. Thermodynamic Properties of Condensed Uranium Dioxide. High Temperature, 2018, 56(5): 652-661.

[2] Ronchi C, Hyland G J. Analysis of recent measurements of the heat capacity of uranium dioxide. Journal of Alloys and Compounds, 1994, 213-214: 159-168.

[3] Bo T, Lan JH, Wang CZ, et al. First-principles study of water reaction and H2 formation on UO2 (111) and (110) single crystal surfaces. The Journal of Physical Chemistry C, 2014, 118(38): 21935-21944.

[4] Margueret A, Balice L, Popa K, et al. Spark plasma sintering of UO2 nanopowders: Pressure, heating rate and current effects. Journal of the European Ceramic Society, 2022, 42(13): 6056-6066.

[5] Dorado B, Amadon B, Freyss M, et al. DFT+ U calculations of the ground state and metastable states of uranium dioxide. Physical Review B—Condensed Matter and Materials Physics, 2009, 79(23): 235125.

[6] Sanati M, Albers R, Lookman T, et al. Elastic constants, phonon density of states, and thermal properties of UO2. Physical Review B—Condensed Matter and Materials Physics, 2011, 84(1): 014116.

[7] Waber J. A review of the corrosion of uranium and its alloys. Los Alamos Scientific Laboratory, Los Alamos, New Mexico, 1952.

[8] WineR K, Colmenares C, Smith R, et al. Interaction of water vapor with clean and oxygen-covered uranium surfaces. Surface Science, 1987, 183(1-2): 67-99.

[9] Le Guyadec F, Génin X, Bayle JP, et al. Pyrophoric behaviour of uranium hydride and uranium powders. Journal of Nuclear Materials, 2010, 396(2): 294-302.

[10] Ablitzer C, Le Guyadec F, Raynal J, et al. Influence of superficial oxidation on the pyrophoric behaviour of uranium hydride and uranium powders in air. Journal of Nuclear Materials, 2013, 432(1): 135-145.

[11] Totemeier TC, Pahl RG, Frank SM. Oxidation kinetics of hydride-bearing uranium metal corrosion products. Journal of Nuclear Materials, 1999, 265(3): 308-320.

[12] Zhai M, Zhang S, Xu W, et al. Review of hydrogen-induced mechanical degradation in uranium and uranium alloys. Journal of Nuclear Materials, 2025, 616: 156102.

[13] Masrukan U, Adi WA, Handoko D, et al. CORROSION CHARACTERISTICS STUDY ON URANIUM AND ITS ALLOYS (U-Nb, U-Zr, AND U-Zr-Nb). Urania: Jurnal Ilmiah Daur Bahan Bakar Nuklir, 2025, 31(1): 35-48.

[14] Kondo T, Beck F, Fontana M. A gas chromatographic study on the kinetics of uranium oxidation in moist environments. Corrosion, 1974, 30(9): 330-341.

[15] Kondo T, Verink E, Beck F, et al. Gas chromatographic and gravimetric studies of uranium oxidation mechanism. Corrosion, 1964, 20(10): 314t-320t.

[16] Grimes J, Morris J. Uranium corrosion studies. Part I. An optical method for following oxide formation: Atomic Weapons Research Establishment, Aldermaston, England (United Kingdom), 1965.

[17] Xiong Bitao. Experimental Study on the Reaction of Uranium with Water Vapor. China Academy of Engineering Physics, 2003.

[18] Allen GC, Tucker PM, Lewis RA. X-ray photoelectron spectroscopy study of the initial oxidation of uranium metal in oxygen+ water-vapour mixtures. Journal of the Chemical Society, Faraday Transactions 2: Molecular and Chemical Physics, 1984, 80(8): 991-1000.

[19] Donald SB, Stanford JA, Haschke JM, et al. Parabolic oxidation kinetics of a plutonium alloy at room temperature. Corrosion Science, 2021, 187: 109527.

[20] Santon JP. A kinetic study of the reaction of water vapor and carbon dioxide on uranium: CEA Grenoble, 38 (France), 1964.

[21] Wang S, Li H, Li G, et al. The oxidative kinetics of uranium at different stages. Corrosion Science, 2022, 206: 110487.

[22] Chernia Z, Ben-Eliyahu Y, Kimmel G, et al. The initial stage of uranium oxidation: Mechanism of UO2 scale formation in the presence of a native lateral stress field. The Journal of Physical Chemistry B, 2006, 110(46): 23041-23051.

[23] Colby JR L. Kinetics of the reaction of uranium monocarbide with water. Journal of the Less Common Metals, 1966, 10(6): 425-431.

[24] Tiferet E, Zalkind S, Mintz MH, et al. Interactions of water vapor with polycrystalline uranium surfaces – The low temperature regime. Surface Science, 2007, 601(4): 936-940.

[25] Banos A, Scott T. A review of the reaction rates of uranium corrosion in water. Journal of Hazardous Materials, 2020, 399: 122763.

[26] Baker MM, Less L, Orman S. Uranium+ water reaction. Part 1.—Kinetics, products and mechanism. Transactions of the Faraday Society, 1966, 62: 2513-2524.

[27] Xiong Bitao, Meng Daqiao, Yang Weicai, et al. Experimental study on accelerated corrosion of metallic uranium in a water vapor atmosphere. Atomic Energy Science and Technology, 2005, 39(3): 226-231.

[28] Shamir N, Tiferet E, Zalkind S, et al. Interactions of water vapor with polycrystalline uranium surfaces. Surface Science, 2006, 600(3): 657-664.

[29] Manner W L, Lloyd JA, Paffett MT. Reexamination of the fundamental interactions of water with uranium. Journal of nuclear materials, 1999, 275(1): 37-46.
[30] Liu Zhixiao. First-principles study on the adsorption and dissociation characteristics of oxygen-containing gas molecules on uranium surfaces. Hunan University, 2013(4).
[31] Zhu S L, Yang YX, Zhang ZF, et al. Density functional theory study of adsorption of H2O on γ -U(110) surface. Indian Journal of Physics, 2023, 97(8): 2297-2306.
[32] Zhu S, Xie Q, Hu J, et al. Density functional theory (DFT+D3) study on the adsorption of water on the γ -U(100) surface. Physica B: Condensed Matter, 2025, 717: 417841.
[33] Balooch M, Hamza A. Hydrogen and water vapor adsorption on and reaction with uranium. Journal of nuclear materials, 1996, 230(3): 259-270.
[34] Danon A, Koresh J, Mintz M. Temperature programmed desorption characterization of oxidized uranium surfaces: relation to some gas− uranium reactions. Langmuir, 1999, 15(18): 5913-5920.
[35] Li Gan, Yu Huilong, Yin Chen. Adsorption and dissociation of H2O molecules on α -U(001) surfaces. Rare Metals Materials and Engineering, 2014, 43(01): 85-90.
[36] Li H, Ding Q, Gu Y, et al. The initial oxidation behavior of uranium and uranium-titanium alloys in standing storage. Corrosion Science, 2020, 176: 108879.
[37] Haschke JM, Allen TH, Morales LA. Reactions of plutonium dioxide with water and hydrogen – oxygen mixtures: Mechanisms for corrosion of uranium and plutonium. Journal of Alloys and Compounds, 2001, 314(1-2): 78-91.
[38] Hughes AN, Orman S, Picton G. Environmental factors affecting the mechanical properties of uranium: Part 1. The effect of water vapour. Journal of Nuclear Materials, 1969, 33(2): 159-164.
[39] Hughes AN, Orman S, Picton G, et al. Environmental factors affecting the mechanical properties of uranium: Part 2. The mechanism of the water embrittlement of uranium. Journal of Nuclear Materials, 1969, 33(2): 165-172.
[40] Haschke JM, Allen TH, Stakebake JL. Reaction kinetics of plutonium with oxygen, water and humid air: moisture enhancement of the corrosion rate. Journal of Alloys and Compounds, 1996, 243(1): 23-35.
[41] Banos A, Burrows R, Scott T. A review of the mechanisms, reaction products and parameters affecting uranium corrosion in water. Coordination Chemistry Reviews, 2021, 439: 213899.
[42] Mingao Q, Tao W, Chen X, et al. Research Progress on Surface Corrosion of Uranium Materials. Journal of Physics: Conference Series, 2021, 1965(1): 012055.
[43] Haschke JM. Corrosion of uranium in air and water vapor: consequences for environmental dispersal. Journal of alloys and compounds, 1998, 278(1-2): 149-160.
[44] Colmenares C, Howell R, Mccreary T. Oxidation of uranium studied by gravimetric and positron annihilation techniques: Lawrence Livermore National Lab., CA (USA), 1981.
[45] Weirick L, Lynch C. Corrosion resistant coatings for uranium and uranium alloys. Proceedings of the CORROSION 1977. Association for Materials Protection and Performance, San Francisco, CA, 1977, 1-24. DOI: 10.5006/C1977-77027.
[46] Baker MM, Less L, Orman S. Uranium+ water reaction. Part 2.—Effect of oxygen and other gases. Transactions of the Faraday Society, 1966, 62: 2525-2530.
[47] Colmenares C. Oxidation mechanisms and catalytic properties of the actinides. Progress in Solid State Chemistry, 1984, 15(4): 257-364.
[48] Mcgillivray G, Geeson D, Greenwood R. Studies of the kinetics and mechanism of the oxidation of uranium by dry and moist air A model for determining the oxidation rate over a wide range of temperatures and water vapour pressures. Journal of Nuclear Materials, 1994, 208(1-2): 81-97.
[49] Skomurski F, Shuller L, Ewing R, et al. Corrosion of UO2 and ThO2: A quantum-mechanical investigation. Journal of Nuclear Materials, 2008, 375(3): 290-310.
[50] Qu X, He B, Li R, et al. The promotion effect of oxygen on the dissociative adsorption of water to uranium dioxide surface: a GGA+ U study. Journal of Radioanalytical and Nuclear Chemistry, 2018, 317(2): 1013-20.
[51] Qu X, Li RS, He B, et al. Co-adsorption of O2 and H2O on α -uranium (110) surface: A density functional theory study. Chinese Physics B, 2018, 27(7): 076501.
[52] Liu H, Liu F, Zong H, et al. Initial oxidation behavior of α -U and γ -U surfaces. Journal of Nuclear Materials, 2024, 592: 154964.
[53] Bazley S, Petherbridge J, Glascott J. The influence of hydrogen pressure and reaction temperature on the initiation of uranium hydride sites. Solid State Ionics, 2012, 211: 1-4.
[54] Banos AK. Investigation of uranium corrosion in mixed water-hydrogen environments; University of Bristol, 2017.
[55] Owen L, Scudamore R. A microscope study of the initiation of the hydrogen-uranium reaction. Corrosion Science, 1966, 6(11-12): 461-468.
[56] Arkush R, Venkert A, Aizenshtein M, et al. Site related nucleation and growth of hydrides on uranium surfaces. Journal of alloys and compounds, 1996, 244(1-2): 197-205.
[57] Bloch J, Simca F, Kroup M, et al. The initial kinetics of uranium hydride formation studied by a hot-stage microscope technique. Journal of the Less Common Metals, 1984, 103(1): 163-171.
[58] Bloch J, Brami D, Kremner A, et al. Effects of gas phase impurities on the topochemical-kinetic behaviour of uranium hydride development. Journal of the Less Common Metals, 1988, 139(2): 371-383.

[59] Brill M, Bloch J, Mintz M. Experimental verification of the formal nucleation and growth rate equations – initial UH3 development on uranium surface. Journal of alloys and compounds, 1998, 266(1-2): 180-185.
[60] Brill M, Bloch J, Shmariahu D, et al. The incipient kinetics of hydride growth on cerium surfaces. Journal of alloys and compounds, 1995, 231(1-2): 368-375.
[61] Glascott J. Hydrogen & Uranium; Interactions between the first and last naturally occurring elements. Discovery – Sci Tech J of AWE, 2003, 6: 16-27.
[62] Bloch J, Mintz MH. Kinetics and mechanisms of metal hydrides formation—a review. Journal of Alloys and Compounds, 1997, 253: 529-541.
[63] Mintz MH, Bloch J. Evaluation of the kinetics and mechanisms of hybriding reactions. Progress in solid state chemistry, 1985, 16(3): 163-194.
[64] Ben-Eliyahu Y, Brill M, Mintz M. Hydride nucleation and formation of hydride growth centers on oxidized metallic surfaces—kinetic theory. The Journal of chemical physics, 1999, 111(13): 6053-6060.
[65] Harker RM. The influence of oxide thickness on the early stages of the massive uranium – hydrogen reaction. Journal of alloys and compounds, 2006, 426(1-2): 106-117.
[66] Martin M, Gommel C, Borkhart C, et al. Absorption and desorption kinetics of hydrogen storage alloys. Journal of Alloys and Compounds, 1996, 238(1-2): 193-201.
[67] Cohen D, Zeiri Y, Mintz M. Model calculations for hydride nucleation on oxide-coated metallic surfaces: surface- and diffusion-related parameters. Journal of alloys and compounds, 1992, 184(1): 11-23.
[68] Alire R, Mueller B, Peterson CL, et al. Reaction kinetics of uranium and deuterium. The Journal of Chemical Physics, 1970, 52(1): 37-46.
[69] Bedere D, Sans P. Hydridation of the alloy UVsub (0. 095) in the presence or not of the inhibitor CO. J Less-Common Met;(Switzerland), 1983, 91(1).
[70] Teter DF, Hanrahan RJ, Wetteland CJ. Uranium hydride nucleation kinetics: effects of oxide thickness and vacuum outgassing: Los Alamos National Lab., NM (United States), 2001.
[71] Condon J, Larson E. Kinetics of the uranium - hydrogen system. The Journal of Chemical Physics, 1973, 59(2): 855-865.
[72] Taylor CD, Scott Lillard R. Ab-initio calculations of the hydrogen – uranium system: Surface phenomena, absorption, transport and trapping. Acta Materialia, 2009, 57(16): 4707-4715.
[73] Taylor CD, Lookman T, Lillard RS. Ab initio calculations of the uranium – hydrogen system: Thermodynamics, hydrogen saturation of α-U and phase-transformation to UH3. Acta materialia, 2010, 58(3): 1045-1055.
[74] Condon J. Nucleation and growth in the hydriding reaction of uranium. Journal of the Less Common Metals, 1980, 73(1): 105-112.
[75] Jones CP, Scott TB, Petherbridge JR, et al. A surface science study of the initial stages of hydrogen corrosion on uranium metal and the role played by grain microstructure. Solid State Ionics, 2013, 231: 81-86.
[76] Glascott J. A model for the initiation of reaction sites during the uranium – hydrogen reaction assuming enhanced hydrogen transport through thin areas of surface oxide. Philosophical Magazine, 2014, 94(3): 221-241.
[77] Shi P, Shen L, Bai B, et al. Preferred hydride growth orientation of U－0.79 wt.% Ti alloy with β + U2Ti microstructure. Journal of nuclear materials, 2013, 441(1-3): 1-5.
[78] Moreno D, Arkush R, Zalkind S, et al. Physical discontinuities in the surface microstructure of uranium alloys as preferred sites for hydrogen attack. Journal of nuclear materials, 1996, 230(2): 181-186.
[79] Hill M, Schulze R, Bingert J, et al. Filiform-mode hydride corrosion of uranium surfaces. Journal of nuclear materials, 2013, 442(1-3): 106-115.
[80] Scott TB, Allen GC, Findlay I, et al. UD3 formation on uranium: evidence for grain boundary precipitation. Philosophical Magazine, 2007, 87(2): 177-187.
[81] Banos A, Scott TB. Statistical analysis of UH3 initiation using electron back-scattered diffraction (EBSD). Solid State Ionics, 2016, 296: 137-145.
[82] Li L, Zhu M, Li Y, et al. Atomic scale origin of hydrogen induced pitting corrosion in metallic uranium: first principles study of hydrogen behavior at uranium grain boundaries. International Journal of Hydrogen Energy, 2025, 159: 150584.
[83] Banos A, Jones C, Scott T. The effect of work-hardening and thermal annealing on the early stages of the uranium -hydrogen corrosion reaction. Corrosion Science, 2018, 131: 147-155.
[84] Bloch J, Mintz M. Kinetics and mechanism of the UH reaction. Journal of the Less Common Metals, 1981, 81(2): 301-320.
[85] Bloch J. The kinetics of a moving metal hydride layer. Journal of alloys and compounds, 2000, 312(1-2): 135-153.
[86] Yoo M. Slip modes of alpha uranium. Journal of Nuclear Materials, 1968, 26(3): 307-318.
[87] Calhoun C, Wollmershauser J, Brown D, et al. Thermal residual strains in depleted α-U. Scripta materialia, 2013, 69(8): 566-569.
[88] Banos A, Stitt C, Scott T. The effect of sample preparation on uranium hydriding. Corrosion Science, 2016, 113: 91-103.
[89] Jones CP, Scott TB, Petherbridge JR. Structural deformation of metallic uranium surrounding hydride growth sites. Corrosion Science, 2015, 96: 144-151.

[90] Stitt C, Paraskevoulakos C, Harker N, et al. The effects of metal surface geometry on the formation of uranium hydride. Corrosion Science, 2015, 98: 63-71.
[91] Liu Min. First-principles calculations of composition, structure, and properties of uranium-hydrogen binary systems. University of Science and Technology of China, 2019.
[92] Chen L, Ji H, Su B, et al. The role of Nb in enhancing the corrosion resistance of U-Nb alloy to hydrogen. Corrosion Science, 2025, 243: 112594.
[93] Soshnikov A, Lindsey R, Kulkarni A, et al. A reactive molecular dynamics model for uranium/hydrogen containing systems. The Journal of Chemical Physics, 2024, 160(9).
[94] Shiranirad M, English NJ. Development of Machine Learning Atomistic Potential for Molecular Simulation of Hematite‐Water Interfaces. Crystals, 2024, 14(11): 930.
[95] Wen B, Calegari Andrade M F, Liu LM, et al. Water dissociation at the water‐rutile TiO2 (110) interface from ab initio-based deep neural network simulations. Proceedings of the National Academy of Sciences, 2023, 120(2): e2212250120.
[96] Li X, Paier W, Paier J. Machine learning in computational surface science and catalysis: Case studies on water and metal‐oxide interfaces. Frontiers in chemistry, 2020, 8: 601029.